PHYSICAL REVIEW D **80,** 084019 (2009)

Improved gauge driver for the generalized harmonic Einstein system

Lee Lindblom and Béla Szilágyi

Theoretical Astrophysics 350-17, California Institute of Technology, Pasadena, California 91125, USA

(Received 30 April 2009; published 14 October 2009)

A new gauge driver is introduced for the generalized harmonic (GH) representation of Einstein's equation. This new driver allows a rather general class of gauge conditions to be implemented in a way that maintains the hyperbolicity of the combined evolution system. This driver is more stable and effective and, unlike previous drivers, allows stable evolutions using the dual-frame evolution technique. Appropriate boundary conditions for this new gauge driver are constructed, and a new boundary condition for the ''gauge'' components of the spacetime metric in the GH Einstein system is introduced. The stability and effectiveness of this new gauge driver are demonstrated through numerical tests, which impose a new damped-wave gauge condition on the evolutions of single black-hole spacetimes.

DOI: 10.1103/PhysRevD.80.084019 PACS numbers: 04.25.D−, 02.60.Cb, 04.20.Cv, 04.25.dg

I. INTRODUCTION

The gauge (or coordinate) degrees of freedom in the generalized harmonic (GH) form of the Einstein equations are determined by specifying the gauge-source functions H^a. These functions are defined as the results of the covariant scalar-wave operator acting on each of the spacetime coordinates x^a:

$$H^a = \nabla^c \nabla_c x^a. \tag{1}$$

(We use Latin letters from the beginning of the alphabet, $a, b, c, \ldots$, for spacetime indices.) The GH form of Einstein's equations can be represented (somewhat abstractly) as

$$\psi^{cd}\partial_c\partial_d\psi_{ab} + \partial_a H_b + \partial_b H_a = Q_{ab}(H, \psi, \partial\psi), \tag{2}$$

where ψ_{ab} is the spacetime metric, $H_a = \psi_{ab}H^b$, and Q_{ab} represents lower-order terms that depend on H_a, the metric, and its first derivatives. These equations are manifestly hyperbolic whenever H_a is specified as an explicit function of the coordinates and the metric: $H_a = H_a(x, \psi)$. In this case the terms $\partial_a H_b$ appearing in Eq. (2) contain at most first derivatives of the metric. The Einstein equations become, therefore, a set of second-order wave equations for each component of the spacetime metric:

$$\psi^{cd}\partial_c\partial_d\psi_{ab} = \hat{Q}_{ab}(x, \psi, \partial\psi). \tag{3}$$

Thus the Einstein equations are manifestly hyperbolic for any $H_a = H_a(x, \psi)$.

Most of the useful gauge conditions developed by the numerical relativity community over the past several decades cannot, unfortunately, be expressed in the simple form $H_a = H_a(x, \psi)$, unless the full spacetime metric $\psi_{ab} = \psi_{ab}(x)$ is known *a priori*. Many of these conditions (e.g., Bona-Massó slicing or the Γ-driver shift conditions) would require gauge-source functions that depend on the spacetime metric and its first derivatives: $H_a = H_a(x, \psi, \partial\psi)$, cf. Ref. [1]. In this case the terms $\partial_a H_b$ in Eq. (2) would depend on the second derivatives of the metric, ψ_{ab}, and this (generically) destroys the hyperbolicity of the system.

This problem can be overcome by elevating H_a to the status of an independent dynamical field and introducing suitable evolution equations for H_a, which we call gauge drivers [1–3]. One obvious choice is to construct gauge-driver equations that force H_a to evolve toward the desired gauge, e.g., $H_a \to F_a$ where F_a is the target for the selected gauge. To be useful these gauge-driver equations must also make the combined Einstein gauge-driver system hyperbolic. It is fairly easy to construct hyperbolic evolution systems designed to evolve H_a toward any target $F_a(x, \psi, \partial\psi)$ that depends on the spacetime metric and its first derivatives [1]. Many of the gauge conditions found most useful by the numerical relativity community have targets F_a that belong to this class. In most cases however, the coupled Einstein gauge-driver evolution equations are unstable and the evolved H_a does not evolve robustly toward every target F_a in this class for generic evolutions. The Einstein gauge-driver system is very complicated, and there are many opportunities for unstable couplings to develop between the dynamics of the spacetime metric and the dynamics of the gauge field H_a. Some gauge conditions, including certain Bona-Massó slicing conditions and some versions of the Γ-driver shift conditions, have been implemented fairly successfully using gauge drivers of this type in full 3D evolutions of strongly perturbed single black-hole spacetimes [1]. However, we find that even these ''successful'' gauge drivers fail when more complicated simulations are attempted, e.g., evolving a single black hole in a rotating reference frame or evolving black-hole binary systems.

The purpose of this paper is to develop a better gauge driver that overcomes some of these problems. To this end we introduce in Sec. II a new class of ''first-order'' gauge-driver evolution equations, which are considerably simpler than earlier drivers. The dynamical simplicity of these new drivers reduces the internal dynamical degrees of freedom available to H_a (in a sense discussed in more detail in

Sec. II), hence reducing the possibility of unwanted feedback or resonances with the dynamics of the Einstein system. We describe numerical tests of this new gauge-driver system in Sec. III that use a new damped-wave gauge introduced in Appendix A to provide an interesting nontrivial dynamical target F_a. Using this target F_a we perform a series of numerical tests that evolve single black-hole spacetimes with large dynamical gauge perturbations. These tests demonstrate the effectiveness and stability of the new gauge-driver system for single- and dual-coordinate frame evolutions. The strongly perturbed black holes in these tests always evolved into nonsingular time independent states, which suggests that the new damped-wave gauge conditions introduced here may prove to be useful for numerical simulations of more general dynamical black-hole spacetimes as well.

We describe in some detail a number of technical properties of this new gauge-driver system in a series of Appendices. In Appendix B we show that any member of this new class of first-order gauge drivers can be coupled to the GH Einstein system in a way that makes the combined system symmetric hyperbolic. In Appendix C we develop a dual-coordinate frame version of this new gauge-driver system, which is needed to evolve black-hole binary systems, for example. In Appendix D we analyze the evolution of the constraints in the new combined GH Einstein gauge-driver system. We show that the constraints and their evolution equations are the same as those of the pure GH Einstein system, hence the constraint damping properties of the original GH Einstein system are also unchanged. In Appendix E we construct boundary conditions for the gauge-driver system. In most cases these boundary conditions turn out to be the same as those used for the pure GH Einstein system, but their representations in terms of the characteristic fields of the gauge-driver system are different in some cases. We also introduce a new constraint-preserving boundary condition for the gauge components of the spacetime metric in the GH Einstein system.

II. FIRST-ORDER GAUGE DRIVER

The gauge drivers previously introduced for the GH Einstein system [1,2,4] were constructed by elevating the gauge-source function H_a to the status of a dynamical field that is evolved by a second-order wave equation for H_a having the general form,

$$\psi^{cd}\partial_c\partial_d H_a = Q_a(H, \partial H, \psi, \partial\psi). \tag{4}$$

When this type of evolution equation for H_a is used together with the GH Einstein evolution Eq. (2), the combined system is manifestly hyperbolic. The first implementations of this type of gauge driver were fairly successful, allowing a few successful binary black-hole inspiral, merger, and ringdown simulations [2,4]. A disadvantage of these first gauge drivers however is that they were not designed to drive H_a toward a predetermined target F_a, so using them made it difficult or impossible to predict what gauge would ultimately be imposed on the solution. One reason for this ambiguity is the dynamical complexity of the operator used to evolve H_a. Even the homogeneous driver, Eq. (4) with $Q_a = 0$, has a wealth of solutions that are not naturally attracted toward any particular target F_a. So it is not surprising that these first gauge drivers have not been found to be very effective for implementing predetermined gauge conditions or for performing evolutions in generic situations. The goal here is to introduce a gauge driver that drives H_a toward a predetermined gauge specified by F_a more robustly and in more generic situations than was possible with the first gauge drivers of this type [1] based on the complicated second-order wave operator used in Eq. (4).

An ideal gauge driver would determine H_a from an evolution equation like

$$\partial_t H_a = -\mu(H_a - F_a), \tag{5}$$

whose solutions all approach the target gauge-source function F_a exponentially, at a rate determined by the freely specifiable parameter μ. Unfortunately the evolution system formed by combining Eq. (5) with the GH Einstein evolution Eq. (2), does not appear to be hyperbolic. There is a simple generalization of this ideal gauge driver however that can be used with the GH Einstein equations to construct a composite evolution system that is hyperbolic. Let t^a denote the future-directed normal to the constant-t hypersurfaces. Then the first-order gauge driver,

$$t^b\partial_b H_a = -\tilde{\mu}(H_a - F_a), \tag{6}$$

combined with the GH Einstein evolution Eq. (2) turns out to be a hyperbolic system.

We present a proof below that the combined GH Einstein gauge-driver system, Eqs. (2) and (6), is hyperbolic. Before turning to that technical issue in Appendix B however, we point out that the very simple gauge driver, Eq. (6), has some limitations which can be overcome to some extent by a simple modification. To see these limitations we introduce spacetime coordinates, $\{t, x^i\}$, where the time coordinate t labels the leaves in a foliation of spacelike hypersurfaces on which the points are identified by the spatial coordinates x^i. In this coordinate system we use the standard 3 + 1 representation of the spacetime metric, ψ_{ab}:

$$\begin{aligned} ds^2 &= \psi_{ab}dx^a dx^b \\ &= -N^2dt^2 + g_{ij}(dx^i + N^i dt)(dx^j + N^j dt), \end{aligned} \tag{7}$$

where g_{ij} is the intrinsic spatial metric of the constant-t hypersurfaces, and N and N^i are referred to as the lapse and shift, respectively. (We use Latin letters from the middle of the alphabet, $i, j, k, \ldots$, for purely spatial indices.) The unit normal to the constant-t hypersurfaces, t^a, has the 3 + 1 representation $t^a\partial_a = N^{-1}(\partial_t - N^k\partial_k)$ in this notation.

Thus the gauge driver given in Eq. (6) can be written more explicitly in 3 + 1 form as

$$\partial_t H_a - N^k \partial_k H_a = -\mu(H_a - F_a), \tag{8}$$

where $\mu = \tilde{\mu} N$. This gauge driver has the property that H_a is driven toward F_a as seen by observers moving along the world lines of the hypersurface normal t^a. However, at a fixed spatial coordinate, x^i, the quantity $H_a - F_a$ is not necessarily driven to zero. Therefore the evolution of a dynamical spacetime (e.g., a perturbed black hole) using this driver will not evolve toward a time independent state in which $H_a = F_a$. Rather this driver will tend to evolve solutions into states with $N^k \partial_k H_a = \mu(H_a - F_a)$. This gauge may provide a reasonable representation of the spacetime, but it will not be the gauge $H_a = F_a$ the driver was intended to enforce.

This limitation in the gauge driver of Eq. (6) can be overcome by introducing an additional dynamical field, θ_a, defined as

$$\partial_t \theta_a + \eta \theta_a = -\eta N^k \partial_k H_a . \tag{9}$$

or equivalently,

$$\theta_a(t) = -\eta \int_{-\infty}^{t} e^{\eta(t'-t)} N^k \partial_k H_a(t') dt'. \tag{10}$$

The θ_a field is an exponentially weighted time average of $-N^k \partial_k H_a$, which can be used to modify the gauge driver of Eq. (6) [1]:

$$\partial_t H_a - N^k \partial_k H_a = -\mu(H_a - F_a) + \theta_a . \tag{11}$$

All time independent solutions of the first-order gauge driver consisting of Eqs. (9) and (11) must now satisfy the desired gauge condition $H_a = F_a$. Since the gauge-driving parameters η and μ are freely specifiable, they can be chosen to enforce the desired gauge on a time scale shorter than the characteristic time τ on which the spacetime evolves. Thus we expect the desired gauge can be enforced using this driver with reasonable accuracy $H_a \approx F_a$ in any spacetime.

In Sec. III we present numerical tests of this first-order gauge driver that demonstrate how well it succeeds. In a series of Appendices we also present some formal analyses of a variety of mathematical properties of the new gauge driver composed of Eqs. (9) and (11) together with the GH Einstein Eq. (2). In particular we show in Appendix B that this combined GH Einstein gauge-driver system is symmetric hyperbolic. In Appendix C we construct a dual-coordinate frame version of this gauge driver that can be used, for example, in the evolution of binary black-hole spacetimes. In Appendix D we analyze the constraints and the evolution of the constraints in the GH Einstein gauge-driver system. In Appendix E we formulate boundary conditions for the new gauge-driver system.

III. NUMERICAL TESTS

In this section we describe the results of 3D numerical tests of the new GH Einstein gauge-driver system. These tests evolve a Schwarzschild black hole with perturbed lapse and shift using the full coupled nonlinear equations for the GH Einstein gauge-driver system, as described in Sec. II. We measure the stability and effectiveness of the new gauge-driver system as it attempts to drive this single black-hole spacetime from the isotropic maximal-slicing gauge used to specify the initial data to an interesting new damped-wave gauge introduced in Appendix A.

These numerical tests are conducted using the infrastructure of the Caltech/Cornell Spectral Einstein Code (SpEC). This code uses pseudospectral collocation methods, as described, for example, in Refs. [5,6]. We use the generalized harmonic form of the Einstein equations, as described in Ref. [7], together with the new gauge-driver Eqs. (9) and (11). Some of the tests reported here use the dual-coordinate frame version of the new gauge-driver system described in Appendix C. For these dual-frame tests we use the static Schwarzschild coordinates as the "inertial" frame, and a "comoving" frame that rotates uniformly at angular velocity Ω with respect to the inertial frame. The evolution equations for the combined GH Einstein gauge-driver system are integrated in time using the method of lines and the adaptive fifth-order Dormand-Prince integrator [8].

Initial conditions are needed for any evolution of the combined GH Einstein gauge-driver system. These initial data consist of the spacetime metric ψ_{ab}, its time derivative $\partial_t \psi_{ab}$, the gauge-source function H_a, and the time averaging field θ_a. For the tests described here we take the initial spacetime metric ψ_{ab} to be the Schwarzschild geometry plus perturbations as described below. We set the time derivatives of the spatial components of the metric initially to zero, and the time derivatives of the lapse and shift, $\partial_t N$ and $\partial_t N^i$, are chosen to make N and N^i initially time independent. For the dual-frame evolution tests described below, these time derivatives are chosen to make N and the comoving-frame components of N^i time independent initially in the comoving frame. The initial value of H_a is chosen to enforce the gauge constraint, $\mathcal{C}_a = H_a + \Gamma_a = 0$, initially. The value of the time averaging field θ_a is set initially to ensure that its time derivative vanishes, as determined by Eq. (9) or (C6).

For these tests we construct initial data consisting of a Schwarzschild black hole with perturbations in the lapse and shift. For the unperturbed hole we use isotropic spatial coordinates and maximal time slices [9,10]. The unperturbed spatial metric in this representation is given by

$$ds^2 = g_{ij} dx^i dx^j = \left(\frac{R}{r}\right)^2 (dx^2 + dy^2 + dz^2), \tag{12}$$

where $r^2 = x^2 + y^2 + z^2$, and $R(r)$ (the areal radius) satisfies the differential equation,

$$\frac{dR}{dr} = \frac{R}{r}\sqrt{1 - \frac{2M}{R} + \frac{C^2}{R^4}}. \tag{13}$$

The constant M is the mass of the hole, and C is a parameter that specifies the particular maximal slicing. Finally, the unperturbed lapse N and shift N^i for this representation of Schwarzschild are given by

$$N = \sqrt{1 - \frac{2M}{R} + \frac{C^2}{R^4}}, \tag{14}$$

$$N^i = \frac{C\hat{r}^i}{R^2}\left(1 - \frac{2M}{R} + \frac{C^2}{R^4}\right), \tag{15}$$

where $\hat{r}^i$ is the outward directed radial unit vector: $g_{ij}\hat{r}^i\hat{r}^j = 1$.

We perturb this spacetime by changing the initial values of the lapse and shift, and their time derivatives. This type of perturbation changes the spacetime coordinates (or gauge) of the solution, but not its geometry. For these tests we modify the lapse and shift of Eqs. (14) and (15) by adding perturbations of the form

$$\delta N = A \sin(2\pi r/r_0) e^{-(r-r_c)^2/w^2} Y_{lm}, \tag{16}$$

$$\delta N^i = A \sin(2\pi r/r_0) e^{-(r-r_c)^2/w^2} Y_{lm}\hat{r}^i, \tag{17}$$

where Y_{lm} is the standard scalar spherical harmonic. In our numerical tests we use the background metric with $C = 1.73M^2$, and perturbations with $A = 0.01$, $r_c = 15M$, $w = 3M$, $r_0 = 6M$, and $l = 2$, $m = 0$.

These numerical tests are performed using the target gauge-source function for the new damped-wave gauge,

$$F_a = \mu_L \log\left(\frac{g^p}{N}\right) t_a - \mu_S N^{-1} g_{ai} N^i, \tag{18}$$

where μ_L and μ_S are damping parameters, $g = \det g_{ij}$, and p is a constant. This new gauge condition is discussed in some detail in Appendix A. The gauge used to prepare the perturbed Schwarzschild initial data, Eqs. (12)–(17), is very different from the damped-wave gauge condition. It is always difficult to start evolutions in a smooth and convergent way using initial data prepared with a significantly different gauge. To minimize this start-up problem, it is common practice to turn on the new gauge condition gradually. We do this in our gauge-driver system by defining an initial target $F_a^{(0)}$ that is simply the constraint-satisfying H_a of the unperturbed initial data. Except for the perturbation, this is exactly the gauge needed for a time independent evolution of these initial data. We then set the target F_a to

$$F_a = e^{-t^2/T^2} F_a^{(0)} + (1 - e^{-t^2/T^2}) F_a^{DW}, \tag{19}$$

where F_a^{DW} is the target gauge-source function for the damped-wave gauge defined in Eq. (18). This choice for F_a changes the gauge condition from its initial state $F_a^{(0)}$ to the desired F_a^{DW} smoothly and gradually on the time scale T. For the tests discussed here we use $T = 10M$ for the value of this time-blending parameter.

These tests use the damped-wave gauge condition defined in Eq. (18) with damping parameters $\mu_S = \mu_L = 0.1$ and $p = 0.5$. Most of these tests (except as noted below) use the values $\mu = \eta = 16$ for the gauge-driver parameters, used in Eqs. (9) and (11), and the boundary gauge-driver parameter $\mu_B = 1$ used in Eq. (E10). These tests set the constraint damping parameters of the GH Einstein system to the values: $\gamma_0 = \gamma_2 = 2$ and $\gamma_1 = -1$, cf. Ref. [7].

We perform these numerical tests on a computational domain consisting of a spherical shell that extends from $r = 0.78M$ (just inside the horizon in the initial coordinates) to $r = 60M$ (well outside the domain of influence of the initial perturbations). We divide this domain into 16 subdomains, which allows us to distribute the computation over several processors to enhance computational speed. In each subdomain we express each Cartesian component of each dynamical field as a sum of Chebyshev polynomials of r (through order $N_r - 1$) multiplied by scalar spherical harmonics (through order L). The radii of the inner and outer edges of the various subdomains are adjusted to distribute the truncation error during the full time evolution more or less uniformly on the grid. The specific radii of the subdomain boundaries used in these tests are $0.78M$, $1.68M$, and $k \times 4.0M$ for $k = 1, \ldots, 15$.

In the pseudospectral numerical method used here, each Cartesian component of each dynamical field is expanded as a sum of the form

$$u(r, \theta, \varphi) = \sum_{k=0}^{N_r-1} \sum_{\ell=0}^{L} \sum_{m=-\ell}^{\ell} u_{k\ell m} T_k(r) Y_{\ell m}(\theta, \varphi), \tag{20}$$

where the $u_{k\ell m}$ are referred to as the spectral coefficients of the field u. These spectral coefficients must be modified in this method through a process called spectral filtering. We use two types of spectral filtering in these tests. One type affects the angular spectral coefficients, as described in Ref. [5]. This filter sets to zero in each time step the changes in the top four *tensor* spherical harmonic expansion coefficients of each of the dynamical fields. This filtering step is needed to eliminate an instability associated with the inconsistent mixing of tensor spherical harmonics whenever angular derivatives are computed in our approach. In addition we also perform the following radial filtering:

$$\mathcal{F}(u_{k\ell m}) = e^{-[k/\rho(N_r-1)]^p} u_{k\ell m}, \tag{21}$$

where $\mathcal{F}(u_{k\ell m})$ represents the filtered coefficients, before applying outer boundary conditions as described in

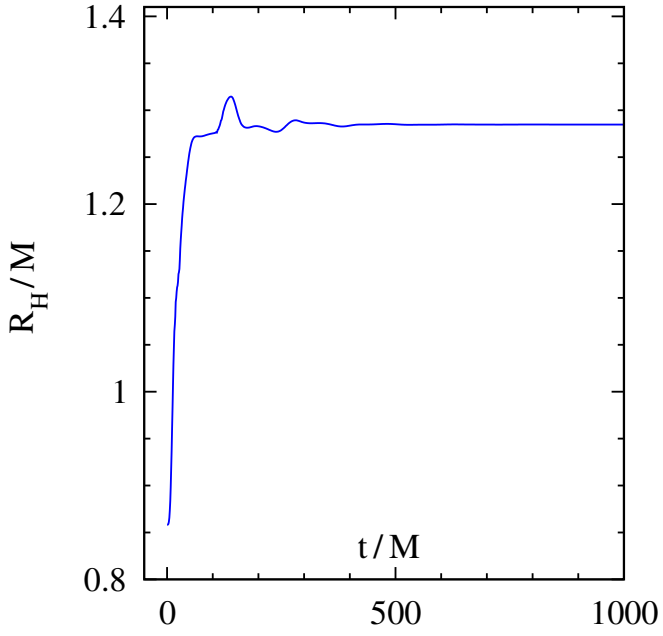

FIG. 1 (color online). Coordinate radius of the apparent horizon of the black hole R_H as it evolves under the effects of the dynamically driven gauge. This test uses a single-frame evolution with gauge-driver parameters $\mu = \eta = 16$.

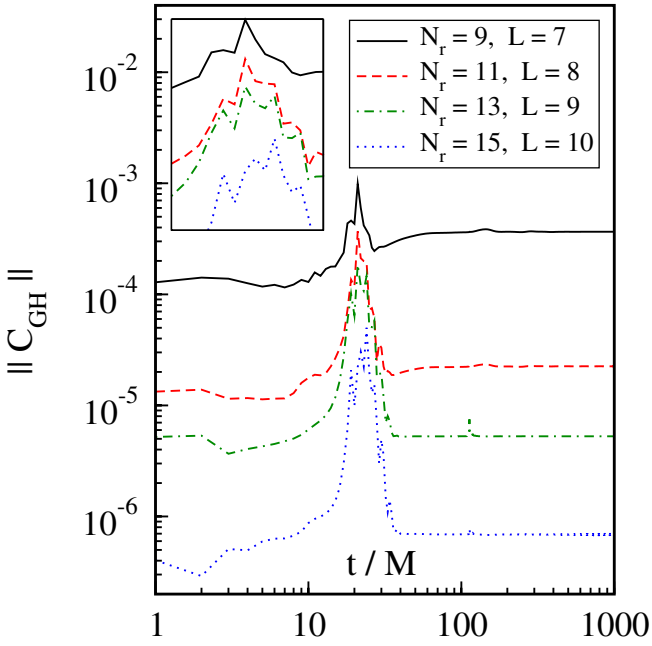

FIG. 2 (color online). Constraints of the GH Einstein system $\|\mathcal{C}_{\rm GH}\|$ for a single-frame evolution of a Schwarzschild black hole with strongly perturbed lapse and shift. This test uses a single-frame evolution with gauge-driver parameters $\mu = \eta = 16$, and several different values of the numerical resolution parameters N_r and L. The small inset graph contains a magnified view of $\|\mathcal{C}_{\rm GH}\|$ during the time interval $15M \leq t \leq 30M$, showing that the solution is convergent during this most dynamical part of the evolution.

Appendix E. For these tests we use $\rho = 0.9$ and $p = 18$, which leaves essentially unchanged the coefficients $u_{k\ell m}$ with $k \lesssim 2(N_r - 1)/3$, while the coefficient of the highest mode, $k = N_r - 1$, is effectively set to zero. This radial filter implements in a smooth way the standard 2/3 filter often used to cure nonlinear aliasing that can occur in spectral evolutions [11,12].

The damped-wave gauge conditions defined by Eq. (18) (and described in Appendix A) are significantly different than those satisfied by the perturbed maximally sliced representation of the Schwarzschild geometry used as initial data for this test. Consequently, the representation of the black hole in our test becomes very dynamical, primarily due to these gauge differences, and also due to the presence of the asymmetric perturbation applied to the lapse and shift. Figure 1 illustrates just how significant these gauge differences are by showing the evolution of the coordinate radius of the apparent horizon R_H of the black hole. In these tests the radius of the apparent horizon R_H grows by 50%, changing from an initial value of $0.86M$ to a final radius of $1.28M$.

Figure 2 illustrates the constraint violations for a single-frame evolution of the GH Einstein gauge-driver system, and demonstrates the stability and convergence of our numerical method. The constraints of the GH Einstein gauge-driver system are identical to those of the GH Einstein system, as discussed in some detail in Appendix D. Therefore we measure constraint violations using the quantity $\|\mathcal{C}_{\rm GH}\|$, the ratio of an L^2 norm of all the GH Einstein constraints divided by an L^2 norm of the derivatives of the dynamical fields. This constraint norm vanishes iff the constraints are satisfied, and has been normalized to be of order unity when constraint violations begin to dominate the solution. This constraint norm was originally introduced to measure constraint violations for the pure GH Einstein system in Eq. (71) of Ref. [7]. The constraint violations become largest and the rate of convergence of the simulations decreases during the time interval $15M \lesssim t \lesssim 30M$ in Fig. 2 when the inward moving gauge perturbation interacts most strongly with the black hole. These results show that the constraints are well satisfied throughout the evolutions, demonstrates that our numerical methods are convergent, and shows that the GH Einstein gauge-driver system is stable over many dynamical time scales. Figure 3 provides another illustration of the stability and the numerical convergence of the GH Einstein gauge-driver system. In this figure we show $|\delta M(t)|/M$ the evolution of the difference between the evolved and the initial mass of the black hole (as determined from the area of its apparent horizon).

Figure 4 demonstrates the effectiveness of the gauge-driver system for this test problem. The difference between the gauge-source function H_a and the target function to which it is being driven, F_a, is measured using the following L^2 norm:

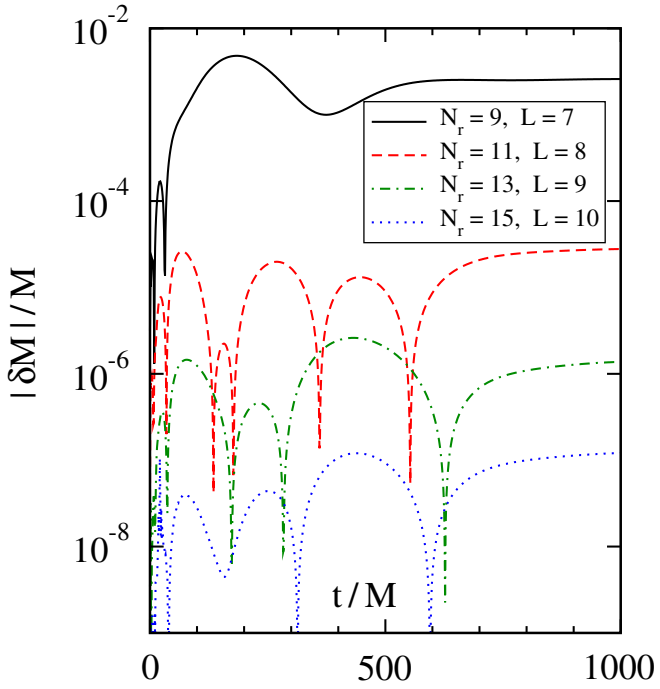

FIG. 3 (color online). Curves show $|\delta M|/M$, the deviations in the mass of the hole from its initial value. This test uses a single-frame evolution with gauge-driver parameters $\mu = \eta = 16$.

$$\frac{\|H - F\|^2}{\|F\|^2} = \frac{\int \sqrt{g} m^{ab} (H_a - F_a)(H_b - F_b) d^3x}{\int \sqrt{g} m^{cd} F_c F_d d^3x}, \quad (22)$$

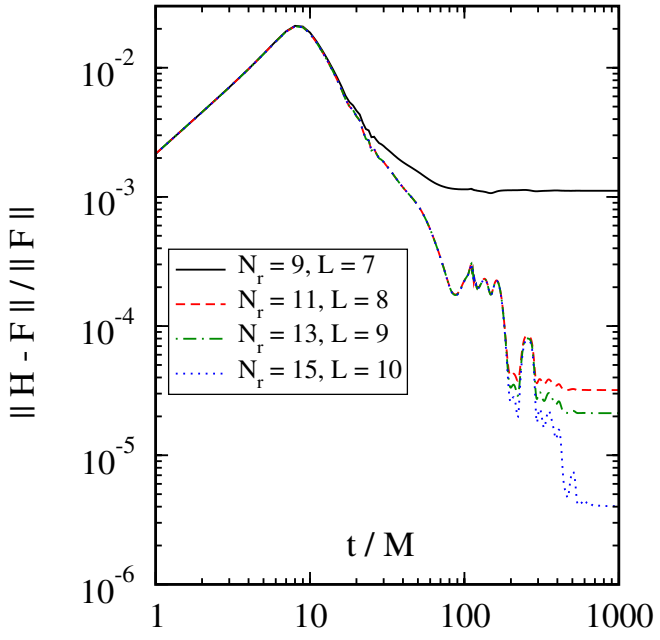

FIG. 4 (color online). Effectiveness of the gauge-driver equation is demonstrated by showing $\|H - F\|/\|F\|$ for an evolution of a Schwarzschild black hole with strongly perturbed lapse and shift. This test uses a single-frame evolution with gauge-driver parameters $\mu = \eta = 16$.

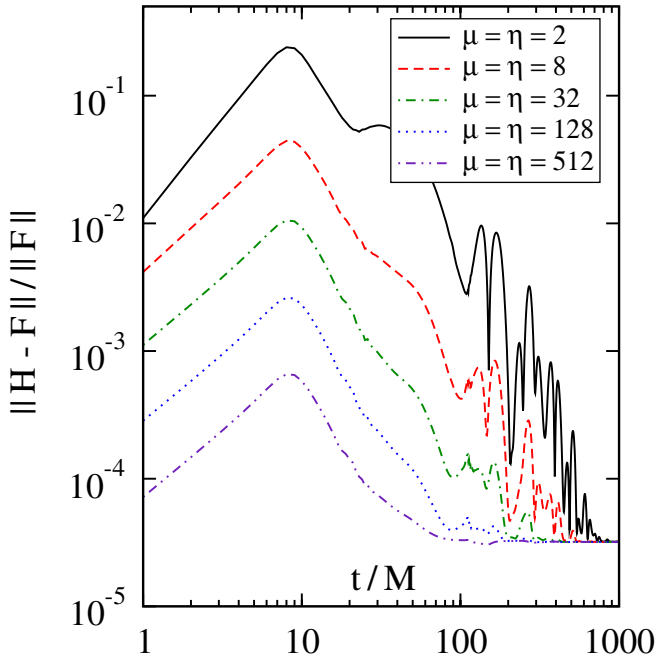

FIG. 5 (color online). Effectiveness of the gauge-driver system is demonstrated for various values of the gauge-driver parameters η and μ. This test uses a dual-frame evolution method with the comoving frame rotating with respect to the inertial frame at angular velocity $\Omega = 1/M$.

where m^{ab} is a positive definite matrix, set to the identity, $m^{ab} = \delta^{ab}$, for these tests. This norm vanishes if and only if the target gauge condition, $H_a = F_a$, is satisfied, and it is scaled so that H_a bears little resemblance to the target F_a whenever it becomes of order unity. Figure 5 shows that the initial mismatch between the gauge of the perturbed black hole and the damped-wave gauge conditions (defined by F_a) causes $\|H - F\|/\|F\|$ to grow initially. But the gauge driver steps in and limits this growth to a maximum of about 0.02 in these evolutions, and then drives $\|H - F\|/\|F\|$ to very small values (depending on the numerical resolution) at late times.

The evolution tests illustrated in Figs. 1–4 were performed using the single-frame version of the gauge-driver system described in Sec. II. Binary black-hole simulations are done with the Caltech/Cornell SpEC code using a dual-coordinate frame formulation of the GH Einstein equations [13]. In this formulation the components of the various tensor fields are defined with respect to a nonrotating inertial-coordinate frame, while the equations for these field components are solved using a comoving coordinate frame that tracks the motions of the black holes. A dual-frame version of the GH Einstein gauge-driver system is developed in Appendix C. We have performed the same perturbed single black-hole evolution tests illustrated in Figs. 1–4 using this dual-frame version of the GH Einstein gauge-driver system. For these tests we use a comoving frame that rotates with respect to the asymptotic inertial

frame at angular velocity $\Omega = 1/M$. (This means that equatorial grid points in this test move at 60 times the speed of light at the outer edge of our computational domain.) The gauge driver used for these evolutions is the hybrid driver described in Appendix C, Eqs. (C10) and (C11). This driver attempts to enforce the comoving-frame gauge condition $H_a = F_a$ in the spacetime region near the black hole, while enforcing the inertial-frame condition $H_{\bar{a}} = F_{\bar{a}}$ near the outer boundary of the computational domain. The transition between these is accomplished by smoothly blending the two conditions at intermediate points using a weight function $w(x)$, cf. Eqs. (C10) and (C11). In regions where $w(x) = 1$, the pure comoving-frame condition is enforced, and where $w(x) = 0$ the pure inertial-frame condition is used. For these numerical tests we use $w(r) = e^{-[r/(0.89R_o)]^{17}}$, where $R_o = 60M$ is the outer radius of the computational domain. This choice accurately enforces the comoving-frame condition in the inner region of the domain where $r \lesssim 2R_o/3$, and the inertial-frame condition at points located very near the outer boundary, $r \approx R_o$.

The graphs of the quantities depicted in Figs. 1–4 for the dual-frame evolution case are almost identical to their single-frame evolution counterparts. So we will not show those graphs again here. Instead we show in Fig. 5 a series of evolutions performed with the dual-frame system in which the effects of varying the gauge-driver parameters μ and η are examined. We see from these results that the gauge-driver system is very effective in driving $H_a \to F_a$ for a wide range of gauge-driver parameters. Evolutions using larger values of the gauge-driver parameters are generally more effective in keeping the quantity $\|H - F\|/\|F\|$ small and driving it quickly toward zero. The gauge-driver system is stable and effective over a rather wide range of parameters, but becomes ineffective when the gauge-driver parameters get smaller than about one, and the system also becomes unstable when the parameters are larger than a few hundred.

ACKNOWLEDGMENTS

We thank Mark Scheel and Keith Matthews for helpful discussions concerning this work. This work was supported in part by grants from the Sherman Fairchild Foundation, by NSF Grants No. DMS-0553302, No. PHY-0601459, and No. PHY-0652995, and by NASA Grant No. NNX09AF97G. Some of the computations for this investigation were performed at the Jet Propulsion Laboratory using computers funded by the JPL Office of the Chief Information Officer.

APPENDIX A: DAMPED-WAVE GAUGE CONDITIONS

Harmonic gauge is defined by the condition that each coordinate x^a satisfies the covariant scalar-wave equation:

$$\nabla^c \nabla_c x^a = H^a = 0. \tag{A1}$$

Harmonic coordinates have proven to be extremely useful for analytical studies of the Einstein equations, but have found only limited success in numerical problems like simulations of complicated highly dynamical black-hole mergers. A likely reason for some of these difficulties is the wealth of ''interesting'' dynamical solutions to the harmonic gauge condition itself, Eq. (A1). Since all ''physical'' dynamical fields are expressed in terms of the coordinates, an ideal gauge condition would limit coordinates to those that are simple, straightforward, dependable, and nonsingular; having ''interesting'' dynamics of their own is *not* a desirable feature for coordinates. We propose to reduce the dynamical range available to harmonic coordinates by adding a damping term to the equation:

$$\nabla^c \nabla_c x^a = \mu_S t^c \partial_c x^a = \mu_S t^a, \tag{A2}$$

where t^a is the future-directed unit normal to the constant-t hypersurfaces. Adding such a damping term to the equations for the spatial coordinates x^i tends to remove extraneous gauge dynamics and drives the coordinates toward solutions of the covariant spatial Laplace equation on the time scale $1/\mu$. Choosing $1/\mu$ to be comparable to (or smaller than) the characteristic time scale of a particular problem should remove any extraneous coordinate dynamics on time scales shorter than the physical time scale. The addition of such a damping term in the time-coordinate equation is not appropriate, however. Such a damped-wave time coordinate is driven toward a constant value, and therefore toward a state in which it fails to be a useful time coordinate at all. It makes sense then to use the damped-wave gauge condition only for the spatial coordinates:

$$\nabla^c \nabla_c x^i = H^i = \mu_S t^i = -\mu_S N^i/N, \tag{A3}$$

where N^i is the shift, and N is the lapse. The appropriate contravariant version of this damped-wave gauge condition is therefore

$$H_a = -\mu_S g_{ai} N^i/N, \tag{A4}$$

where $g_{ab} = \psi_{ab} + t_a t_b$ is the spatial metric.[1]

We point out that the damped-wave gauge condition, Eq. (A4), is very similar to one version of the Γ-driver shift condition adopted recently by several groups using moving puncture evolution methods [15]. It is straightforward to express the covariant wave operator in terms of the $3 + 1$ decomposition of the metric:

$$\nabla^c \nabla_c x^i = -{}^{(3)}\Gamma^i + N^{-2}(\partial_t N^i - N^k \partial_k N^i) + g^{ik}\partial_k \log N, \tag{A5}$$

[1]Frans Pretorius and Matthew Choptuik have recently, independently, proposed adding similar damping terms to the harmonic gauge condition [14].

where ${}^{(3)}\Gamma^i$ is the trace of the Christoffel connection computed from g_{ij}. It follows that the damped-wave shift condition, Eq. (A3), is equivalent to the following condition on the shift:

$$\partial_t N^i - N^k \partial_k N^i + \mu_S N N^i = N^2[{}^{(3)}\Gamma^i - g^{ik}\partial_k \log N]. \tag{A6}$$

In comparison a version of the Γ-driver shift condition, cf. Eq. (26) of Ref. [15], that is currently being used by a number of numerical relativity groups is a very similar condition:

$$\partial_t N^i - N^k \partial_k N^i + \eta N^i = 0.75\, {}^{(3)}\tilde{\Gamma}^i, \tag{A7}$$

where ${}^{(3)}\tilde{\Gamma}^i$ is the trace of the Christoffel connection computed from the conformal metric $\tilde{g}_{ij} = g^{-1/3} g_{ij}$. This version of the Γ-driver shift condition is therefore a certain conformal damped-wave equation for the spatial coordinates.

While the damped-wave gauge is a poor choice for the time coordinate, the idea of imposing a gauge that uses the dissipative properties of the damped-wave equation to suppress extraneous gauge dynamics is attractive. The lapse is the rate of change of proper time with respect to the time coordinate (as measured by an observer moving along t^a), so choosing a gauge in which the lapse satisfies a damped-wave equation seems like the appropriate time-domain analog of the damped-wave spatial gauge condition. To find the appropriate expression for $t^a H_a$ that leads to such an equation, we note that the gauge constraint $H_a + \Gamma_a = 0$ implies that $t^a H_a$ is given by

$$t^a H_a = -K - t^a \partial_a \log N, \tag{A8}$$

where $K = g^{ij} K_{ij}$ is the trace of the extrinsic curvature of the constant-t hypersurfaces. Using the definition of K, this condition can be also be written in the form

$$t^a H_a = t^a \partial_a \log\left(\frac{\sqrt{g}}{N}\right) - N^{-1}\partial_k N^k, \tag{A9}$$

where $g = \det g_{ij}$ is the spatial volume element. One frequent symptom of the failure of simpler gauge conditions in binary black-hole simulations is an explosive growth in g in the spacetime region near the black-hole horizons. This suggests choosing the gauge condition,

$$t^a H_a = -\mu_L \log\left(\frac{\sqrt{g}}{N}\right), \tag{A10}$$

for $\mu_L > 0$, which tends to suppress any growth in $\sqrt{g}/N$ as a consequence of the constraint, Eq. (A9).

To determine how this gauge condition, Eq. (A10), effects the evolution of the lapse, we note that the time derivative of K is determined by the Einstein evolution equations:

$$t^a \partial_a K = K_{ij} K^{ij} - N^{-1} D^i D_i N, \tag{A11}$$

where D_i is the spatial covariant derivative compatible with g_{ij}. Combining this expression with Eq. (A8) gives an equation for the time derivative of $t^a H_a$,

$$N t^b \partial_b (t^a H_a) = -t^b \partial_b (t^a \partial_a N) + D^i D_i N + N^{-1}(t^a \partial_a N)^2 - N K_{ij} K^{ij}, \tag{A12}$$

which is a wave operator acting on the lapse. When the gauge condition in Eq. (A10) is enforced, it equates this wave operator to the following expression:

$$N t^b \partial_b (t^a H_a) = \mu_L t^a \partial_a N - \tfrac{1}{2}\mu_L N t^a \partial_a \log g. \tag{A13}$$

The first term on the right side of Eq. (A13) is a standard damping term for the lapse wave equation, while the second term plays the role of an additional "source." The motivation for including the particular dependence on g in Eq. (A13) is provided by the argument leading to Eq. (A10); however, this dependence can easily be generalized without changing the term's fundamental lapse-damping property by setting

$$t^a H_a = -\mu_L \log\left(\frac{g^p}{N}\right), \tag{A14}$$

where p is a constant. The case $p = 0.5$ corresponds to Eq. (A10), while $p = 0$ is a pure lapse-damping gauge without the extra source term.

Combining this new lapse condition, Eq. (A14), with the damped-wave spatial coordinate condition, Eq. (A4), gives the target gauge-source function for our full damped-wave gauge condition:

$$F_a = \mu_L \log\left(\frac{g^p}{N}\right) t_a - \mu_S N^{-1} g_{ai} N^i. \tag{A15}$$

This gauge condition depends only on the spacetime metric ψ_{ab}, so it could be implemented directly in the GH Einstein system by setting $H_a = F_a$. However, it can also be implemented with the new GH Einstein gauge-driver system introduced in Sec. II, where it can be used as a nontrivial test of the new gauge driver. Numerical evolutions of strongly perturbed single black-hole spacetimes using the $p = 0.5$ version of this gauge and the new GH Einstein gauge-driver system are described in Sec. III.

APPENDIX B: HYPERBOLICITY

The hyperbolicity of an evolution system consisting of some first-order equations, like our new gauge-driver Eqs. (9) and (11), and some second-order equations, like the GH Einstein Eq. (2), is most easily analyzed by converting all the equations to first-order form. The spectral evolution code that we use to perform our numerical simulations is rather sensitive to ill-posed evolution problems. So we generally perform our numerical simulations by evolving first-order systems of equations where hyperbolicity is easier to analyze and where boundary conditions are easier to construct. Mixed systems like the combined

Einstein and gauge-driver equations can be converted to first-order form by introducing additional dynamical fields for the first derivatives of those fields satisfying second-order equations. Convenient choices of the needed additional fields for the GH Einstein system are $\Pi_{ab} = -t^c \partial_c \psi_{ab}$ and $\Phi_{iab} = \partial_i \psi_{ab}$. The evolution equations for these fields, $\{\psi_{ab}, \Pi_{ab}, \Phi_{iab}\}$, then become a first-order representation of the GH Einstein system:

$$\partial_t \psi_{ab} - (1+\gamma_1) N^k \partial_k \psi_{ab} = -N \Pi_{ab} - \gamma_1 N^i \Phi_{iab}, \tag{B1}$$

$$\begin{aligned} &\partial_t \Pi_{ab} - N^k \partial_k \Pi_{ab} + N g^{ki} \partial_k \Phi_{iab} - \gamma_1 \gamma_2 N^k \partial_k \psi_{ab} \\ &\quad + 2N \partial_{(a} H_{b)} \\ &= -\tfrac{1}{2} N t^c t^d \Pi_{cd} \Pi_{ab} - N t^c \Pi_{ci} g^{ij} \Phi_{jab} \\ &\quad + 2N \psi^{cd} (g^{ij} \Phi_{ica} \Phi_{jdb} - \Pi_{ca} \Pi_{db} - \psi^{ef} \Gamma_{ace} \Gamma_{bdf}) \\ &\quad + N \gamma_0 [2 \delta^c_{\ (a} t_{b)} - \psi_{ab} t^c] (H_c + \psi^{ef} \Gamma_{cef}) \\ &\quad + 2N \Gamma^c_{ab} H_c - \gamma_1 \gamma_2 N^i \Phi_{iab}, \end{aligned} \tag{B2}$$

$$\begin{aligned} &\partial_t \Phi_{iab} - N^k \partial_k \Phi_{iab} + N \partial_i \Pi_{ab} - N \gamma_2 \partial_i \psi_{ab} \\ &\quad = \tfrac{1}{2} N t^c t^d \Phi_{icd} \Pi_{ab} + N g^{jk} t^c \Phi_{ijc} \Phi_{kab} - N \gamma_2 \Phi_{iab}, \end{aligned} \tag{B3}$$

cf. Eqs. (35)–(37) of Ref. [7]. In these equations N, N^i, and g_{ij} are the standard 3 + 1 representation of ψ_{ab} given in Eq. (7); t^a is the future-directed timelike unit normal; Γ^c_{ab} is the Christoffel connection associated with ψ_{ab}; and γ_0, γ_1, and γ_2 are parameters multiplying constraints, introduced because they help damp away small constraint violations. This representation of the GH Einstein equations together with the gauge driver introduced above, Eqs. (9) and (11), is a first-order evolution system which can be represented abstractly as

$$\partial_t u^\alpha + A^{k\alpha}_{\ \ \beta} \partial_k u^\beta = B^\alpha. \tag{B4}$$

For the combined GH Einstein gauge-driver system, the collection of dynamical fields is $u^\alpha = \{\psi_{ab}, \Pi_{ab}, \Phi_{iab}, H_a, \theta_a\}$, where Greek letters are used for indices that enumerate the dynamical fields.

The hyperbolicity of a first-order evolution system, such as Eq. (B4), is determined by the properties of the characteristic matrix $A^{k\alpha}_{\ \ \beta}$. We define the left eigenvectors $e^{\hat{\alpha}}_{\ \ \alpha}$ and their associated eigenvalues $v_{(\hat{\alpha})}$ of the characteristic matrix in the following way:

$$e^{\hat{\alpha}}_{\ \ \beta} n_k A^{k\beta}_{\ \ \alpha} = v_{(\hat{\alpha})} e^{\hat{\alpha}}_{\ \ \alpha}, \tag{B5}$$

where n_k denotes a spacelike unit vector; accented Greek letters, $\hat{\alpha}, \ldots$, are used to enumerate distinct linearly independent eigenvectors. The eigenvalues, $v_{(\hat{\alpha})}$, are often referred to as the characteristic speeds of the system. A first-order evolution system is strongly hyperbolic at a point in spacetime if there exists a complete set of eigenvectors for each n_k at that point. In this case the matrix of eigenvector components $e^{\hat{\alpha}}_{\ \ \alpha}$ is nondegenerate, i.e., $\det e^{\hat{\alpha}}_{\ \ \alpha} \neq 0$. The projections of the dynamical fields onto the eigenvectors, $u^{\hat{\alpha}} = e^{\hat{\alpha}}_{\ \ \alpha} u^\alpha$, provide an alternate complete set of dynamical fields, which play an important role in strongly hyperbolic systems. For example, the characteristic fields, $u^{\hat{\alpha}}$, are those on which appropriate boundary conditions must be placed for these systems.

It is fairly straightforward to work out the characteristic eigenvalues and eigenvectors, and the associated characteristic fields, for the combined GH Einstein gauge-driver system:

$$u^{\hat{0}}_{ab} = \psi_{ab}, \tag{B6}$$

$$u^{\hat{1}^\pm}_{ab} = \Pi_{ab} \pm n^i \Phi_{iab} - \gamma_2 \psi_{ab} \pm n_a H_b \pm n_b H_a, \tag{B7}$$

$$u^{\hat{2}}_{iab} = P^k_i \Phi_{kab}, \tag{B8}$$

$$u^{\hat{3}}_a = H_a, \tag{B9}$$

$$u^{\hat{4}}_a = \theta_a + \eta H_a, \tag{B10}$$

where $P^k_i = \delta^k_i - n_i n^k$. We see that the coupling between the GH Einstein and gauge-driver systems increases the number of characteristic fields, and also transforms the characteristic fields of the pure GH Einstein system. This means that the theory of the boundary conditions for the GH Einstein system will have to be completely reexamined. We also note that the covector n_a is a spatial unit normal, which is orthogonal to the timelike unit normal t_a. This implies that the spatial components of n_a are the usual components of the spatial normal covector n_i while the time component n_t must be given by $n_t = n_k N^k$. These conditions ensure that $t^a n_a = 0$ and $n^a n_a = n^k n_k = 1$.

The characteristic speeds, $v_{(\hat{\alpha})}$, associated with the combined GH Einstein gauge-driver system are as follows: the fields $u^{\hat{0}}_{ab}$ have coordinate characteristic speed $-(1+\gamma_1) n_k N^k$, the fields $u^{\hat{1}^\pm}_{ab}$ have speed $-n_k N^k \pm N$, the fields $u^{\hat{2}}_{iab}$ and $u^{\hat{3}}_a$ have speed $-n_k N^k$, and the fields $u^{\hat{4}}_a$ have speed zero. On boundary points each characteristic field (computed with the outward directed unit normal to the boundary n_k) must be supplied with a boundary condition if and only if its associated characteristic speed is negative. The appropriate boundary conditions for the combined GH Einstein gauge-driver system are discussed in some detail in Appendix E.

The inverse transformation between dynamical and characteristic fields for the combined GH Einstein gauge-driver system is

$$\psi_{ab} = u^{\hat{0}}_{ab}, \tag{B11}$$

$$\Pi_{ab} = \tfrac{1}{2}(u^{\hat{1}+}_{ab} + u^{\hat{1}-}_{ab}) + \gamma_2 u^{\hat{0}}_{ab}, \tag{B12}$$

$$\Phi_{iab} = \tfrac{1}{2} n_i (u^{\hat{1}+}_{ab} - u^{\hat{1}-}_{ab}) + u^{\hat{2}}_{iab} - n_i (n_a u^{\hat{3}}_b + n_b u^{\hat{3}}_a), \tag{B13}$$

$$H_a = u^{\hat{3}}_a, \tag{B14}$$

$$\theta_a = u^{\hat{4}}_a - \eta u^{\hat{3}}_a. \tag{B15}$$

Since this transformation is invertible, the combined first-order GH Einstein gauge-driver evolution system is strongly hyperbolic.

A first-order evolution system, Eq. (B4), is called symmetric hyperbolic if there exists a symmetric positive definite matrix on the space of dynamical fields, $S_{\alpha\beta}$, that symmetrizes the characteristic matrices: $S_{\alpha\gamma}A^{k\gamma}{}_{\beta} \equiv A^k_{\alpha\beta} = A^k_{\beta\alpha}$. Symmetric hyperbolic systems provide a natural "energy," $E = \int S_{\alpha\beta} u^\alpha u^\beta d^3x$, and are better behaved than strongly hyperbolic systems for initial-boundary value problems. Symmetric hyperbolicity is therefore a desirable property for gauge-driver systems to have. It is fairly straightforward to show that the combined GH Einstein gauge-driver system of Eqs. (2), (9), and (11) has a symmetrizer given by

$$\begin{aligned} dS^2 &= S_{\alpha\beta} du^\alpha du^\beta \\ &= m^{ab}[\Lambda_\psi^2 m^{cd} d\psi_{ac} d\psi_{bd} + \Lambda_H^2 dH_a dH_b + \Lambda_\theta^2 (d\theta_a + \eta dH_a)(d\theta_b + \eta dH_b)] \\ &\quad + m^{ab} m^{cd} [g^{ij} (d\Phi_{iac} + 2 g_{ia} dH_c)(d\Phi_{jbd} + 2 g_{jb} dH_d) + (d\Pi_{ac} - \gamma_2 d\psi_{ac})(d\Pi_{bd} - \gamma_2 d\psi_{bd})]. \end{aligned} \tag{B16}$$

This symmetrizer is positive definite as long as m^{ab} is a positive definite symmetric tensor, and the (real) scalars Λ_ψ, Λ_H, and Λ_θ are nonvanishing. Therefore the gauge-driver system of Eqs. (2), (9), and (11) is symmetric hyperbolic.

APPENDIX C: DUAL-COORDINATE FRAMES

We have found that using two different coordinate systems simultaneously is a very useful numerical technique, when performing numerical evolutions of binary black-hole spacetimes [13]. This method allows us to choose one set of coordinates, x^a thought of as "comoving," to track (approximately) the motion of the black holes, and a second set, $x^{\bar{a}}$ thought of as "inertial," fixed (approximately) to a nonrotating frame at infinity. We evaluate the components of the various dynamical fields using tensor bases defined by the inertial $x^{\bar{a}}$ coordinates, while the evolution equations are solved for those inertial-frame field components $u^{\bar{\alpha}}$ as functions of the moving x^a coordinates. This use of dual-coordinate frames minimizes the size of the various field components and their time derivatives better than any single-frame coordinate choice.

The single-frame GH Einstein gauge-driver equations, introduced in Sec. II, written in terms of inertial-frame quantities are given by

$$\partial_{\bar{t}} H_{\bar{a}} - \bar{N}^{\bar{k}} \partial_{\bar{k}} H_{\bar{a}} = -\mu (H_{\bar{a}} - F_{\bar{a}}) + \theta_{\bar{a}}, \tag{C1}$$

$$\partial_{\bar{t}} \theta_{\bar{a}} + \eta \bar{N}^{\bar{k}} \partial_{\bar{k}} H_{\bar{a}} = -\eta \theta_{\bar{a}}. \tag{C2}$$

These equations, together with the inertial-frame representations of the Einstein system, can be converted to dual-frame form in a straightforward way using the prescription developed in Ref. [13]. Under this recipe, a first-order evolution system for inertial-frame components, $u^{\bar{\alpha}}$,

$$\partial_{\bar{t}} u^{\bar{\alpha}} + A^{\bar{k}\,\bar{\alpha}}{}_{\bar{\beta}} \partial_{\bar{k}} u^{\bar{\beta}} = B^{\bar{\alpha}}, \tag{C3}$$

is converted into the dual-frame system

$$\partial_t u^{\bar{\alpha}} + [\partial_{\bar{t}} x^i \delta^{\bar{\alpha}}{}_{\bar{\beta}} + \partial_{\bar{k}} x^i A^{\bar{k}\,\bar{\alpha}}{}_{\bar{\beta}}] \partial_i u^{\bar{\beta}} = B^{\bar{\alpha}}, \tag{C4}$$

simply by changing independent variables: $\partial_{\bar{t}} = \partial_t + \partial_{\bar{t}} x^i \partial_i$ and $\partial_{\bar{k}} = \partial_{\bar{k}} x^i \partial_i$. The quantities $\partial_{\bar{t}} x^i \equiv \partial x^i / \partial \bar{t}$ and $\partial_{\bar{k}} x^i \equiv \partial x^i / \partial x^{\bar{k}}$ are the nontrivial parts of the Jacobian of the transformation relating the two coordinate frames. These coordinate transformations are assumed to be given *a priori*.

The straightforward conversion of the GH Einstein gauge-driver system from its inertial single-frame form, (C1) and (C2), to dual-frame form may not always be the most effective choice however. The single-frame evolution equation for $H_{\bar{a}}$, Eq. (C1), is designed to drive $H_{\bar{a}} \to F_{\bar{a}}$ at fixed values of the inertial coordinates. A binary black-hole spacetime, however, can have rapid time variations in the field components when evaluated at fixed inertial coordinates, e.g., at points lying near the black-hole trajectories. The gauge-driver system will not be very efficient in accurately enforcing the desired gauge under these very dynamical conditions. In contrast the moving coordinates, x^a, are chosen to track (approximately) the motion of the holes, so the fields expressed as functions of the moving coordinates are far less time dependent. A moving-frame version of the gauge-driver would therefore be more effective enforcing the desired gauge, $H_{\bar{a}} = F_{\bar{a}}$, in many situations. In this case it makes sense to modify the evolution equation for $H_{\bar{a}}$ in a way that ensures the moving-frame

components of H_a are driven to the intended targets: $H_a \rightarrow F_a$. The appropriate moving-frame gauge-driver equations are simply Eqs. (9) and (11) interpreted now as moving-frame equations:

$$\partial_t H_a - N^k \partial_k H_a = -\mu(H_a - F_a) + \theta_a, \tag{C5}$$

$$\partial_t \theta_a + \eta N^k \partial_k H_a = -\eta \theta_a. \tag{C6}$$

It is straightforward to reexpress these equations in terms of inertial-frame quantities:

$$\partial_{\bar{t}} H_{\bar{a}} - \bar{N}^{\bar{k}} \partial_{\bar{k}} H_{\bar{a}} = -\mu(H_{\bar{a}} - F_{\bar{a}}) + \theta_{\bar{a}} + (\partial_{\bar{t}} \partial_{\bar{a}} x^a - \bar{N}^{\bar{k}} \partial_{\bar{k}} \partial_{\bar{a}} x^a) \partial_a x^{\bar{b}} H_{\bar{b}}, \tag{C7}$$

$$\begin{aligned} &\partial_{\bar{t}} \theta_{\bar{a}} + \partial_t x^{\bar{k}} \partial_{\bar{k}} \theta_{\bar{a}} + \eta(\bar{N}^{\bar{k}} + \partial_t x^{\bar{k}}) \partial_{\bar{k}} H_{\bar{a}} \\ &= -\eta \theta_{\bar{a}} + (\partial_{\bar{t}} \partial_{\bar{a}} x^a + \partial_t x^{\bar{k}} \partial_{\bar{k}} \partial_{\bar{a}} x^a) \partial_a x^{\bar{b}} \theta_{\bar{b}} \\ &\quad + \eta(\bar{N}^{\bar{k}} + \partial_t x^{\bar{k}})(\partial_{\bar{k}} \partial_{\bar{a}} x^a) \partial_a x^{\bar{b}} H_{\bar{b}}, \end{aligned} \tag{C8}$$

where $\partial_{\bar{a}} = \partial_{\bar{a}} x^a \partial_a$ transforms the derivatives, $H_{\bar{a}} = \partial_{\bar{a}} x^a H_a$ and $\theta_{\bar{a}} = \partial_{\bar{a}} x^a \theta_a$ transform the field components, and the inertial-frame shift $\bar{N}^{\bar{k}}$ is related to the moving-frame shift N^k by

$$N^k = (\bar{N}^{\bar{k}} + \partial_t x^{\bar{k}}) \partial_{\bar{k}} x^k. \tag{C9}$$

In some circumstances it may be advantageous to apply the inertial-frame version of the gauge driver, Eqs. (C1) and (C2), in one region of spacetime, while applying the moving-frame version, Eqs. (C1) and (C2), in another. For example, in a binary black-hole simulation it might be appropriate to impose the moving-frame version of the gauge driver in the very dynamical region of spacetime near the black holes, while imposing the inertial-frame version in the more quiescent asymptotic region far from the holes. Therefore, to accommodate this possibility we introduce the following hybrid gauge-driver system that simply interpolates between the two:

$$\partial_{\bar{t}} H_{\bar{a}} - \bar{N}^{\bar{k}} \partial_{\bar{k}} H_{\bar{a}} = -\mu(H_{\bar{a}} - F_{\bar{a}}) + \theta_{\bar{a}} + w(\partial_{\bar{t}} \partial_{\bar{a}} x^a - \bar{N}^{\bar{k}} \partial_{\bar{k}} \partial_{\bar{a}} x^a) \partial_a x^{\bar{b}} H_{\bar{b}}, \tag{C10}$$

$$\begin{aligned} &\partial_{\bar{t}} \theta_{\bar{a}} + w \partial_t x^{\bar{k}} \partial_{\bar{k}} \theta_{\bar{a}} + \eta(\bar{N}^{\bar{k}} + w \partial_t x^{\bar{k}}) \partial_{\bar{k}} H_{\bar{a}} \\ &= -\eta \theta_{\bar{a}} + w(\partial_{\bar{t}} \partial_{\bar{a}} x^a + \partial_t x^{\bar{k}} \partial_{\bar{k}} \partial_{\bar{a}} x^a) \partial_a x^{\bar{b}} \theta_{\bar{b}} \\ &\quad + w\eta(\bar{N}^{\bar{k}} + \partial_t x^{\bar{k}})(\partial_{\bar{k}} \partial_{\bar{a}} x^a) \partial_a x^{\bar{b}} H_{\bar{b}}. \end{aligned} \tag{C11}$$

In these equations the smooth weight function w is specified *a priori*, with $w = 0$ in the spacetime region where an inertial-frame gauge driver is needed, and $w = 1$ in the regions where a moving-frame gauge driver is required. The dual-frame version of this hybrid gauge-driver system is obtained by combining these equations with the inertial-frame Einstein system, Eqs. (B1)–(B3), and using the dual-frame conversion technique summarized in Eqs. (C3) and (C4).

Since the hybrid gauge-driver Eqs. (C10) and (C11) do not have the same principal parts as their single-frame counterparts, we must consider again the hyperbolicity of the combined GH Einstein plus hybrid gauge-driver system. Fortunately, we find that this system is still strongly hyperbolic, and the characteristic fields are just Eqs. (B6)–(B10) expressed in terms of inertial-frame field components. The characteristic speeds associated with these fields are modified somewhat however: The fields $u^{\hat{0}}_{\bar{a}\,\bar{b}}$ have inertial-coordinate characteristic speed $-(1 + \gamma_1) n_{\bar{k}} \bar{N}^{\bar{k}}$, the fields $u^{\hat{1}\pm}_{\bar{a}\,\bar{b}}$ have speeds $-n_{\bar{k}} \bar{N}^{\bar{k}} \pm \bar{N}$, the fields $u^{\hat{2}}_{\bar{i}\,\bar{a}\,\bar{b}}$ and $u^{\hat{3}}_{\bar{a}}$ have speed $-n_{\bar{k}} \bar{N}^{\bar{k}}$, and $u^{\hat{4}}_{\bar{a}}$ has the speed $w n_{\bar{k}} \partial_t x^{\bar{k}}$. In these expressions $\bar{N}$ and $\bar{N}^{\bar{k}}$ refer to the inertial-frame lapse and shift, respectively. The comoving-frame characteristic speeds are obtained from the inertial-frame speeds by adding $-n_{\bar{k}} \partial_t x^{\bar{k}}$. This hybrid gauge-driver system is also symmetric hyperbolic with the same symmetrizer, Eq. (B16), interpreted as an expression in terms of inertial-frame field components.

APPENDIX D: CONSTRAINTS

This Appendix investigates the constraints of the new GH Einstein gauge-driver system. These constraints and (somewhat surprisingly) their evolution equations turn out to be identical to those of the pure GH Einstein system. This means that the constraint-preserving boundary conditions derived for the pure GH Einstein system are also appropriate for the combined GH Einstein gauge-driver system, although care must be taken to enforce them on the correct characteristic fields of the combined system. This section presents the groundwork for the detailed discussion of boundary conditions in Appendix E.

The primary constraint of the GH Einstein system is the gauge constraint, $\mathcal{C}_a$, which can be written in terms of the first-order dynamical fields:

$$\mathcal{C}_a = H_a + g^{ij} \Phi_{ija} + t^b \Pi_{ba} - \tfrac{1}{2} g^i_a \psi^{bc} \Phi_{ibc} - \tfrac{1}{2} t_a \psi^{bc} \Pi_{bc}. \tag{D1}$$

There are no extra constraints from the addition of the first-order gauge-driver fields H_a and θ_a. In the pure GH Einstein system the gauge-source function H_a is assumed to be a prescribed function of the spacetime coordinates x^a and the four-metric ψ_{ab}: $H_a = H_a(x, \psi)$. In contrast H_a is elevated to the status of an independent dynamical field that is evolved according to Eq. (11) in the combined GH Einstein gauge-driver system. We need to determine whether the evolution of the GH constraint fields is affected by the introduction of this gauge-driver equation. In addition we need to find the characteristic constraint fields to determine what constraint-preserving boundary conditions are needed for the new combined system.

The basic GH Einstein system, Eqs. (B1)–(B3), is, as before, just a representation of the four-dimensional covariant Einstein equation:

$$R_{ab} = \nabla_{(a}\mathcal{C}_{b)} - \gamma_0[t_{(a}\mathcal{C}_{b)} - \tfrac{1}{2}\psi_{ab}t^c\mathcal{C}_c], \tag{D2}$$

where R_{ab} is the Ricci curvature, and ∇_a is the covariant derivative associated with ψ_{ab}. Consequently, the evolution equation for $\mathcal{C}_a$ is determined by the Bianchi identities for the four-dimensional Ricci tensor, which can be written as the second-order wave equation:

$$0 = \nabla^c\nabla_c\mathcal{C}_a - 2\gamma_0\nabla^b[t_{(b}\mathcal{C}_{a)}] + \mathcal{C}^b\nabla_{(a}\mathcal{C}_{b)} - \tfrac{1}{2}\gamma_0 t_a\mathcal{C}^b\mathcal{C}_b\,. \tag{D3}$$

This equation is identical to that obtained for the pure GH Einstein system [7], because its derivation does not depend on how the H_a field is evolved.

Constraint-preserving boundary conditions are designed to prohibit the influx of constraint violations through the boundaries of the computational domain. In order to fix the incoming constraint fields, the characteristic fields of the constraint evolution system must be identified. This is done most easily by transforming the second-order constraint evolution Eq. (D3) to first-order form. To do this we introduce new constraint fields representing the first derivatives of $\mathcal{C}_a$. Thus we define new constraint fields $\mathcal{F}_a$ and $\mathcal{C}_{ia}$ that satisfy

$$\mathcal{F}_a \approx t^c\partial_c\mathcal{C}_a = N^{-1}(\partial_t\mathcal{C}_a - N^i\partial_i\mathcal{C}_a), \tag{D4}$$

$$\mathcal{C}_{ia} \approx \partial_i\mathcal{C}_a\,, \tag{D5}$$

where $\approx$ indicates equality up to terms proportional to the gauge constraint $\mathcal{C}_a$ and the first-order GH Einstein constraint $\mathcal{C}_{iab} \equiv \partial_i\psi_{ab} - \Phi_{iab}$. The following expressions for $\mathcal{F}_a$ and $\mathcal{C}_{ia}$ accomplish this in a way that keeps the form of the constraint evolution system as simple as possible:

$$\begin{aligned}\mathcal{F}_a \equiv{}& \tfrac{1}{2}g^i_a\psi^{bc}\partial_i\Pi_{bc} - g^{ij}\partial_i\Pi_{ja} - g^{ij}t^b\partial_i\Phi_{jba} + g^i_a\Phi_{ijb}g^{jk}\Phi_{kcd}\psi^{bd}t^c - \tfrac{1}{2}g^i_a\Phi_{ijb}g^{jk}\Phi_{kcd}\psi^{cd}t^b + \tfrac{1}{2}t_a\psi^{bc}g^{ij}\partial_i\Phi_{jbc}\\
&- \tfrac{1}{4}t_ag^{ij}\Phi_{icd}\Phi_{jbe}\psi^{cb}\psi^{de} - \tfrac{1}{2}t_ag^{ij}g^{mn}\Phi_{imc}\Phi_{njd}\psi^{cd} + g^{ij}\Phi_{icd}\Phi_{jba}\psi^{bc}t^d + \tfrac{1}{4}t_a\Pi_{cd}\Pi_{be}\psi^{cb}\psi^{de} - g^{ij}H_i\Pi_{ja}\\
&- t^bg^{ij}\Pi_{bi}\Pi_{ja} - \tfrac{1}{4}g^i_a\Phi_{icd}t^ct^d\Pi_{be}\psi^{be} + \tfrac{1}{2}t_a\Pi_{cd}\Pi_{be}\psi^{ce}t^dt^b + g^i_a\Phi_{icd}\Pi_{be}t^ct^b\psi^{de} - \tfrac{1}{2}g^{ij}\Phi_{icd}t^ct^d\Pi_{ja}\\
&- g^{ij}\Phi_{iba}t^b\Pi_{je}t^e + g^i_a\Phi_{icd}H_b\psi^{bc}t^d + t_ag^{ij}\partial_iH_j + \gamma_2(g^{id}\mathcal{C}_{ida} - \tfrac{1}{2}g^i_a\psi^{cd}\mathcal{C}_{icd}) + \tfrac{1}{2}t_ag^{ij}H_i\Phi_{jcd}\psi^{cd}\\
&+ \tfrac{1}{2}t_a\Pi_{cd}\psi^{cd}H_bt^b - g^{ij}H_i\Phi_{jba}t^b - g^i_at^b\partial_iH_b - t_ag^{ij}\Phi_{ijc}H_d\psi^{cd},\end{aligned} \tag{D6}$$

$$\begin{aligned}\mathcal{C}_{ia} \equiv{}& g^{jk}\partial_j\Phi_{ika} - \tfrac{1}{2}g^j_a\psi^{cd}\partial_j\Phi_{icd} - \tfrac{1}{2}t_a\psi^{cd}\partial_i\Pi_{cd} + t^b\partial_i\Pi_{ba} + \partial_iH_a + \tfrac{1}{2}g^j_a\Phi_{jcd}\Phi_{ief}\psi^{ce}\psi^{df} + \tfrac{1}{2}g^{jk}\Phi_{jcd}\Phi_{ike}\psi^{cd}t^et_a\\
&- g^{jk}g^{mn}\Phi_{jma}\Phi_{ikn} + \tfrac{1}{2}\Phi_{icd}\Pi_{be}t_a(\psi^{cb}\psi^{de} + \tfrac{1}{2}\psi^{be}t^ct^d) - \Phi_{icd}\Pi_{ba}t^c(\psi^{bd} + \tfrac{1}{2}t^bt^d) + \tfrac{1}{2}\gamma_2(t_a\psi^{cd} - 2\delta^c_at^d)\mathcal{C}_{icd}\,.\end{aligned} \tag{D7}$$

We note that, while $\mathcal{F}_a$ is defined as the time derivative of $\mathcal{C}_a$, the expression in Eq. (D6) contains no time derivatives. The constraint fields are functions of the fundamental dynamical fields of the system u^α. Any time derivatives of the constraint fields are determined by the time derivatives of these fundamental fields through the evolution equations of the system. When the time derivatives of the expression for $\mathcal{C}_a$ in Eq. (D1) are evaluated, and the time derivatives of $\{\psi_{ab}, \Pi_{ab}, \Phi_{iab}\}$ are replaced with the expressions from the basic GH Einstein system, Eqs. (B1)–(B3), we find that the occurrences of ∂_tH_a cancel one another. Thus the expression for $\mathcal{F}_a$ does not depend on how H_a is evolved, and it is valid for both the pure GH Einstein system and the new first-order gauge-driver system. To complete the GH constraint evolution system we need to add the GH Einstein constraint $\mathcal{C}_{iab}$,

$$\mathcal{C}_{iab} = \partial_i\psi_{ab} - \Phi_{iab}\,, \tag{D8}$$

and the closely related $\mathcal{C}_{ijab}$, defined by

$$\mathcal{C}_{ijab} = 2\partial_{[i}\Phi_{j]ab} = 2\partial_{[j}\mathcal{C}_{i]ab}\,. \tag{D9}$$

The complete collection of constraints for the GH Einstein gauge-driver evolution system is the set $c^I \equiv \{\mathcal{C}_a, \mathcal{F}_a, \mathcal{C}_{ia}, \mathcal{C}_{iab}, \mathcal{C}_{ijab}\}$ defined in Eqs. (D1) and (D6)–(D9). (We use upper case Latin indices to enumerate the constraint fields.) The constraints c^I depend on the dynamical fields $u^\alpha = \{\psi_{ab}, \Pi_{ab}, \Phi_{iab}, H_a, \theta_a\}$ and their spatial derivatives ∂_ku^α. We have evaluated these constraint evolution equations using the new GH Einstein gauge-driver system and have verified that they can be written in the abstract form,

$$\partial_tc^I + A^{kI}{}_J(u)\partial_kc^J = B^I{}_J(u, \partial u)c^J, \tag{D10}$$

where $A^{kI}{}_J$ and $B^I{}_J$ may depend on the dynamical fields u^α and their spatial derivatives ∂_ku^α. The evolution of the constraint fields c^I turns out to be completely determined by the GH Einstein Eqs. (B1)–(B3) alone without any use of the gauge-driver Eqs. (9) and (11). While the constraint fields $\mathcal{C}_a$, $\mathcal{F}_a$, and $\mathcal{C}_{ia}$ depend on H_a and ∂_kH_a, the time derivatives of these constraints are determined without using the evolution equation for H_a, Eq. (11). There is a remarkable cancellation between the explicit time derivatives of H_a appearing in $\partial_t\mathcal{F}_a$ and $\partial_t\mathcal{C}_{ia}$, and the time

derivatives of H_a introduced when the $\partial_t \Pi_{ta}$ terms are replaced in these expressions using the GH evolution Eq. (B2). Thus the constraint evolution system for the first-order gauge-driver system does not depend at all on the gauge-driver Eqs. (9) and (11). This constraint evolution system is identical to the pure GH Einstein constraint evolution system given in Ref. [7], and is both strongly and symmetric hyperbolic.

Since the constraint evolution equations for the GH Einstein gauge-driver system are identical to those of the pure GH Einstein system, the characteristic constraint fields $c^{\hat{I}}$ are also identical. The boundary conditions needed to ensure no influx of constraint violations will also be the same therefore. As we have seen in Appendix B however, the characteristic dynamical fields $u^{\hat{\alpha}}$ of the two systems are not the same, so the detailed expressions for the needed boundary conditions in the two systems will be different. So we recall here the expressions for the characteristic constraint fields $c^{\hat{I}}$ from Ref. [7]:

$$c_a^{\hat{0}\pm} = \mathcal{F}_a \mp n^k \mathcal{C}_{ka}, \tag{D11}$$

$$c_a^{\hat{1}} = \mathcal{C}_a, \tag{D12}$$

$$c_{ia}^{\hat{2}} = P^k{}_i \mathcal{C}_{ka}, \tag{D13}$$

$$c_{iab}^{\hat{3}} = \mathcal{C}_{iab}, \tag{D14}$$

$$c_{ijab}^{\hat{4}} = \mathcal{C}_{ijab}. \tag{D15}$$

The characteristic constraint fields $c_a^{\hat{0}\pm}$ have coordinate characteristic speeds $-n_l N^l \pm N$, the fields $c_a^{\hat{1}}$ have speed 0, the fields $c_{ia}^{\hat{2}}$ and $c_{ijab}^{\hat{4}}$ have speed $-n_l N^l$, and the fields $c_{iab}^{\hat{3}}$ have speed $-(1+\gamma_1) n_l N^l$. Boundary conditions must be placed on the incoming characteristic dynamical fields $u^{\hat{\alpha}}$ that (among other things) fix the incoming characteristic constraint fields $c^{\hat{I}}$ to zero. These (and other) needed boundary conditions are discussed next in Appendix E.

APPENDIX E: BOUNDARY CONDITIONS

A boundary condition is required for each characteristic field $u^{\hat{\alpha}}$ of the GH Einstein gauge-driver system, at each boundary point where the characteristic speed $v_{(\hat{\alpha})}$ associated with that field is negative.

The characteristic fields $u_{ab}^{\hat{0}}$, Eq. (B6), have speed $-(1+\gamma_1) n_k N^k$ and may require boundary conditions at some boundary points. Since the constraints and the constraint evolution equations of the GH Einstein gauge-driver system are identical to those of the pure GH Einstein system, we can employ the same approach to constructing constraint-preserving boundary conditions. The constraint characteristic field $c_{iab}^{\hat{3}}$, Eq. (D14), is related to the characteristic field $u_{ab}^{\hat{0}}$ by the expression

$$n^i c_{iab}^{\hat{3}} \approx d_\perp u_{ab}^{\hat{0}}, \tag{E1}$$

where $d_\perp u^{\hat{\alpha}}$ denotes the characteristic projection of the normal derivatives of $u^{\hat{\alpha}}$, i.e., $d_\perp u^{\hat{\alpha}} \equiv e^{\hat{\alpha}}{}_\beta n^k \partial_k u^\beta$, with $e^{\hat{\alpha}}{}_\beta$ defined in Eq. (B5). Here (and throughout this Appendix) $\approx$ implies that algebraic terms and terms involving tangential derivatives of the fields (e.g. $P_i^k \partial_k u^\alpha$) have not been displayed. We note that the constraint field $c_{iab}^{\hat{3}}$ has the same characteristic speed as $u_{ab}^{\hat{0}}$. Hence a constraint-preserving boundary condition for $c_{iab}^{\hat{3}}$ is needed whenever $u_{ab}^{\hat{0}}$ needs a boundary condition. The identity relating $u_{ab}^{\hat{0}}$ to $c_{iab}^{\hat{3}}$, Eq. (E1), provides the way to formulate this boundary condition by prescribing the value of $d_\perp u_{ab}^{\hat{0}}$.

A convenient way has been found [7] to impose constraint-preserving boundary conditions for fields like $u_{ab}^{\hat{0}}$ that are related to an incoming constraint field through an expression like Eq. (E1). The characteristic projection of the time derivatives of these fields u^α, $d_t u^{\hat{\alpha}} \equiv e^{\hat{\alpha}}{}_\beta \partial_t u^\beta$, are set in the following way at the boundary:

$$d_t u^{\hat{\alpha}} = D_t u^{\hat{\alpha}} + v_{(\hat{\alpha})} (d_\perp u^{\hat{\alpha}} - d_\perp u^{\hat{\alpha}}|_{BC}). \tag{E2}$$

In this expression the terms $D_t u^{\hat{\alpha}}$ represent the projections of the right sides of the evolution system, Eqs. (9), (11), and (B1)–(B3), so the characteristic projections of the evolution equations at nonboundary points would simply be $d_t u^{\hat{\alpha}} = D_t u^{\hat{\alpha}}$. The term $d_\perp u^{\hat{\alpha}}|_{BC}$ is the value to which $d_\perp u^{\hat{\alpha}}$ is to be fixed on the boundary. This form of the boundary condition replaces all of the $d_\perp u^{\hat{\alpha}}$ that appears in $D_t u^{\hat{\alpha}}$ with $d_\perp u^{\hat{\alpha}}|_{BC}$. Applying this method to the $u_{ab}^{\hat{0}}$ field, we arrive at the desired constraint-preserving boundary condition for this field:

$$d_t u_{ab}^{\hat{0}} = D_t u_{ab}^{\hat{0}} - (1+\gamma_1) n_j N^j n^k c_{kab}^{\hat{3}}. \tag{E3}$$

This boundary condition is the same in the new GH Einstein gauge-driver system as in the pure GH Einstein system [7].

The characteristic field $u_{iab}^{\hat{2}}$, Eq. (B8), has speed $-n_k N^k$, and so this field may require a boundary condition on some boundary points. The constraint characteristic field $c_{ijab}^{\hat{4}}$, Eq. (D15), has the same characteristic speed, and hence it is natural to use the boundary condition on $u_{iab}^{\hat{2}}$ to prevent the influx of this constraint. Conveniently, there is an identity relating $u_{iab}^{\hat{2}}$ and $c_{ijab}^{\hat{4}}$:

$$n^i c_{ikab}^{\hat{4}} \approx d_\perp u_{kab}^{\hat{2}}. \tag{E4}$$

This identity is identical in the GH Einstein gauge driver and the pure GH Einstein systems [7]. So we follow the strategy of Eq. (E2), and use the following constraint-preserving boundary condition for $u_{iab}^{\hat{2}}$:

$$d_t u^{\hat{2}}_{kab} = D_t u^{\hat{2}}_{kab} - n_l N^l n^i P^j{}_k c^{\hat{4}}_{ijab}. \tag{E5}$$

The characteristic field $u^{\hat{3}}_a$, Eq. (B9), also has speed $-n_k N^k$, and so it may require a boundary condition on some boundary points. We have identified two possibilities for this boundary condition. First, the H_a field is part of the basic gauge constraint Eq. (D1). So one possible boundary condition for $u^{\hat{3}}_a$ is simply to enforce this constraint on the boundary:

$$u^{\hat{3}}_a = -g^{ij}\Phi_{ija} - t^b \Pi_{ba} + \tfrac{1}{2} g^i_a \psi^{bc}\Phi_{ibc} + \tfrac{1}{2} t_a \psi^{bc}\Pi_{bc}. \tag{E6}$$

Another possibility is to use a boundary condition on $u^{\hat{3}}_a$ that enforces the desired gauge condition $H_a = F_a$ on the boundary:

$$u^{\hat{3}}_a = F_a. \tag{E7}$$

These boundary conditions could be imposed as Dirichlet conditions in the forms given above using penalty methods. Alternatively, we could impose these conditions using Bjorhus methods as a driver condition on the boundary value of the time derivative of the characteristic field,

$$d_t u^{\hat{\alpha}} = -\mu_B (u^{\hat{\alpha}} - u^{\hat{\alpha}}|_{BC}). \tag{E8}$$

The parameter μ_B sets the time scale on which the boundary value of $u^{\hat{\alpha}}$ is driven to its target value. The Bjorhus version of the boundary condition in Eq. (E6) is therefore

$$d_t u^{\hat{3}}_a = -\mu_B \mathcal{C}_a, \tag{E9}$$

while the Bjorhus version of Eq. (E7) is

$$d_t u^{\hat{3}}_a = -\mu_B (H_a - F_a). \tag{E10}$$

In most of our numerical tests, we find that the Eq. (E10) version of this boundary condition is more effective.

The characteristic field $u^{\hat{4}}_a$, Eq. (B10), has characteristic speed 0 in the single-frame evolution system, and hence does not need a boundary condition in that case. In the dual-frame system the characteristic speed changes to $w n_{\bar{k}} \partial_t x^{\bar{k}}$, so this field might need a boundary condition under some conditions. We have generally chosen weight functions w and dual-frame maps $\partial_t x^{\bar{k}}$ that avoid the need for a boundary condition on this field. But if that cannot be done, it is probably best to choose the boundary value of θ_a so that $\partial_t \theta_a = 0$ on the boundary. This condition leads to the following Dirichlet type boundary condition for $u^{\hat{4}}_a$:

$$u^{\hat{4}}_a = \eta H_a - N^k \partial_k H_a. \tag{E11}$$

Boundary conditions are rarely needed for the $u^{\hat{1}+}_{ab}$ fields, i.e., only when the boundary of the computational domain moves outward at superluminal speeds. In contrast, boundary conditions are almost always needed for the $u^{\hat{1}-}_{ab}$ fields. These boundary conditions split naturally into three types that have been called gauge boundary conditions, constraint-preserving boundary conditions, and physical boundary conditions [7,16]. These three different types of boundary conditions are imposed on the parts of $u^{\hat{1}-}_{ab}$ selected by the three mutually orthogonal projection tensors:

$$P^{(G)cd}_{ab} = -[k_a k_b l^{(c} + k_a \delta_b{}^{(c} + k_b \delta_a{}^{(c}] l^{d)}, \tag{E12}$$

$$P^{(C)cd}_{ab} = \tfrac{1}{2} P_{ab} P^{cd} - 2 l_{(a} P_{b)}{}^{(c} k^{d)} + l_a l_b k^c k^d, \tag{E13}$$

$$P^{(P)cd}_{ab} = P_a{}^{(c} P^{d)}_b - \tfrac{1}{2} P_{ab} P^{cd}. \tag{E14}$$

In these expressions k^a and l^a represent the ingoing and outgoing null vectors, respectively, that are related to the timelike and outgoing spacelike unit normal vectors, t^a and n^a, by

$$k^a = \frac{1}{\sqrt{2}}(t^a - n^a), \tag{E15}$$

$$l^a = \frac{1}{\sqrt{2}}(t^a + n^a). \tag{E16}$$

Similarly g_{ab} represents the spatial three-metric and P_{ab} the projection onto the two-dimensional spatial boundary surface:

$$g_{ab} = \psi_{ab} + t_a t_b, \tag{E17}$$

$$P_{ab} = \psi_{ab} + t_a t_b - n_a n_b. \tag{E18}$$

Finally, we note that the projection tensors $P^{(G)cd}_{ab}$, $P^{(C)cd}_{ab}$, and $P^{(P)cd}_{ab}$ are complete in the sense that

$$\delta_a{}^{(c} \delta_b{}^{d)} = P^{(G)cd}_{ab} + P^{(C)cd}_{ab} + P^{(P)cd}_{ab}. \tag{E19}$$

We now discuss the boundary conditions appropriate for the three independent projections of the $u^{\hat{1}-}_{ab}$ fields.

1. Gauge boundary conditions

The term gauge boundary conditions is used to describe the boundary conditions on the $P^{(G)cd}_{ab}$ projection of $u^{\hat{1}-}_{ab}$ [7]. From the structure of the $P^{(G)cd}_{ab}$ projection tensor, we see that these are in effect boundary conditions on the $u^{\hat{1}-}_{ab} l^b$ fields. Writing out the definition of $u^{\hat{1}-}_{ab}$, we see that

$$u^{\hat{1}-}_{ab} l^b = \Pi_{ab} l^b - n^i \Phi_{iab} l^b - \gamma_2 l_a - n_a H_b l^b - \frac{1}{\sqrt{2}} H_a. \tag{E20}$$

The $u^{\hat{1}\pm}_{ab}$ characteristic fields determine the time and the spatial derivatives of ψ_{ab} normal to the boundary. So these gauge boundary conditions on $u^{\hat{1}-}_{ab} l^b$ can be thought of as fixing the $\Pi_{ab} l^b$ components of Π_{ab}. Previously the gauge boundary condition on $u^{\hat{1}-}_{ab} l^b$ has been set by freezing the value of this projection of the characteristic field,

$P^{(G)cd}_{ab} d_t u^{\hat{1}-}_{cd} = 0$ [7], or by imposing a Sommerfeld-like boundary condition on this projection of $u^{\hat{1}-}_{ab}$ [17].

Here we present a new gauge boundary condition for $u^{\hat{1}-}_{ab} l^b$ obtained by setting the target boundary value of $\Pi_{ab} t^b$ to the value it would have if the gauge constraint were satisfied exactly. The components of $\Pi_{ab} t^b$ enter the gauge constraint, $\mathcal{C}_a$, through the identity

$$\Pi_{ab} t^b = (\delta_a{}^b - t_a t^b)(\mathcal{C}_b - H_b - g^{ij}\Phi_{ijb} + \tfrac{1}{2} g^i_b \psi^{cd}\Phi_{icd} + \tfrac{1}{2} t_b g^{ij}\Pi_{ij}). \tag{E21}$$

So using Eq. (E21) we set

$$\begin{aligned}\Pi_{ab} t^b|_{BC} &= (\delta_a{}^b - t_a t^b)(-H_b - g^{ij}\Phi_{ijb} + \tfrac{1}{2} g^i_b \psi^{cd}\Phi_{icd} + \tfrac{1}{2} t_b g^{ij}\Pi_{ij}) \\ &= \Pi_{ab} t^b - (\delta_a{}^b - t_a t^b)\mathcal{C}_b .\end{aligned} \tag{E22}$$

Using this expression in the equation for $u^{\hat{1}-}_{ab} l^b$ in Eq. (E20), we find the expression for the target boundary value of $u^{\hat{1}-}_{ab} l^b$ to be

$$u^{\hat{1}-}_{ab} l^b|_{BC} = u^{\hat{1}-}_{ab} l^b - \frac{1}{\sqrt{2}}(\delta_a{}^b - t_a t^b)\mathcal{C}_b . \tag{E23}$$

This boundary condition can either be imposed as a Dirichlet condition by penalty methods, or as a boundary-driver condition by Bjorhus methods using Eq. (E8). The Bjorhus version of this new gauge boundary condition is

$$\begin{aligned}P^{(G)cd}_{ab} d_t u^{\hat{1}-}_{cd} &= -\mu_B P^{(G)cd}_{ab}(u^{\hat{1}-}_{cd} - u^{\hat{1}-}_{cd}|_{BC}) \\ &= \frac{\mu_B}{\sqrt{2}}(k_a k_b l^c + k_a \delta_b{}^c + k_b \delta_a{}^c) \\ &\quad \times (\delta_c{}^d - t_c t^d)\mathcal{C}_d .\end{aligned} \tag{E24}$$

2. Constraint-preserving boundary conditions

The term constraint-preserving boundary conditions is used to describe the boundary conditions on the $P^{(C)cd}_{ab}$ projection of $u^{\hat{1}-}_{ab}$. These boundary conditions have been constructed to enforce the incoming components of the constraint characteristic fields $c^{\hat{0}}_a = 0$, defined in Eq. (D11), at the boundary. For the pure GH Einstein system, it was shown that

$$\begin{aligned}c^{\hat{0}-}_a &\approx \sqrt{2}[k^{(c}\psi^{d)}{}_a - \tfrac{1}{2} k_a \psi^{cd}] \\ &\quad \times n^k \partial_k(\Pi_{cd} - n^i \Phi_{icd} - \gamma_0 \psi_{cd}).\end{aligned} \tag{E25}$$

For the case of the pure GH Einstein system, this gives an expression for $c^{\hat{0}-}_a$ in terms of the normal derivative of $u^{\hat{1}-}_{ab}$, and so can be used to construct a boundary condition using Eq. (E2). For the new GH Einstein gauge driver considered here, the $u^{\hat{1}-}_{ab}$ characteristic fields include the additional terms $-n_{(a} H_{b)}$. In the derivation of Eq. (E25) from Eqs. (D6) and (D7), the terms involving spatial derivatives of H_a were treated as being prescribed, and so were counted as some of the (many) algebraic terms not displayed. Since H_a has been elevated to the status of a dynamical field in the new first-order gauge-driver system, however, these terms can no longer be ignored. It turns out that the $\partial_k H_a$ terms in Eqs. (D6) and (D7) give the following extra contributions to Eq. (E25):

$$\begin{aligned}c^{\hat{0}-}_a &\approx \sqrt{2}[k^{(c}\psi^{d)}{}_a - \tfrac{1}{2} k_a \psi^{cd}] \\ &\quad \times n^k \partial_k(\Pi_{cd} - n^i \Phi_{icd} - \gamma_0 \psi_{cd} - n_c H_d - n_d H_c) \\ &\approx \sqrt{2}[k^{(c}\psi^{d)}{}_a - \tfrac{1}{2} k_a \psi^{cd}] d_\perp u^{\hat{1}-}_{cd} .\end{aligned} \tag{E26}$$

Using this expression in Eq. (E2), we then arrive at the needed boundary condition for the constraint-preserving components of $u^{\hat{1}-}_{ab}$:

$$\begin{aligned}P^{(C)cd}_{ab} d_t u^{\hat{1}-}_{cd} &= P^{(C)cd}_{ab} D_t u^{\hat{1}-}_{cd} + \sqrt{2}(N + n_j N^j) \\ &\quad \times [l_{(a} P_{b)}{}^c - \tfrac{1}{2} P_{ab} l^c - \tfrac{1}{2} l_a l_b k^c] c^{\hat{0}-}_c .\end{aligned} \tag{E27}$$

These boundary conditions have the same form as those derived previously for the pure GH Einstein system [7]. Here, however, the characteristic field $u^{\hat{1}-}_{ab}$ has a different meaning, since it depends explicitly on the H_a field in the GH Einstein gauge-driver case.

3. Physical boundary conditions

The term physical boundary condition is used to describe the boundary condition on the $P^{(P)cd}_{ab}$ projection of $u^{\hat{1}-}_{ab}$ [7]. This projection corresponds to the transverse traceless components of the metric field, and so describes the physical gravitational-wave degrees of freedom of the system. In the vacuum region far away from compact sources, the gravitational-wave degrees of freedom are described by the propagating components of the Weyl curvature tensor. The characteristic fields, $w^{\pm}_{ab}$, representing these incoming and outgoing wave degrees of freedom, respectively, of the Weyl tensor, are given by

$$w^{\pm}_{ab} = P^{(P)cd}_{ab}(t^e \mp n^e)(t^f \mp n^f) C_{cedf} . \tag{E28}$$

It is straightforward to show that the incoming gravitational-wave characteristic field w^{-}_{ab} depends on the normal derivatives of the dynamical fields at the boundary by the expression

$$w^{-}_{ab} \approx P^{(P)cd}_{ab} n^k \partial_k(\Pi_{cd} - n^i \Phi_{icd}), \tag{E29}$$

where $\approx$ denotes that algebraic terms and terms depending on tangential derivatives of the dynamical fields are not shown. The derivation of this expression depends on the fact that the physical projection $P^{(P)cd}_{ab}$ annihilates terms like $P^{(P)cd}_{ab}\psi_{cd} = 0$ and $P^{(P)cd}_{ab} n_{(c} H_{d)} = 0$. Therefore the principal part of w^{-}_{ab} depends on the normal derivative of $u^{\hat{1}-}_{ab}$:

$$w^-_{ab} \approx P^{(P)cd}_{ab} d_\perp u^{\hat{1}-}_{cd}. \quad \text{(E30)}$$

This is the same expression (up to terms proportional to constraints) that is satisfied in the pure GH Einstein system case [7], where the gauge-source functions are prescribed: $H_a = H_a(x, \psi)$. But here the characteristic field $u^{\hat{1}-}_{ab}$ has a somewhat different meaning. The lowest-order physical boundary condition is designed to enforce the no-incoming wave condition $w^-_{ab} = 0$ at the boundary. It does this by using Eq. (E30) to replace the normal derivative of $u^{\hat{1}-}_{ab}$ which appears in the Einstein evolution equation for $u^{\hat{1}-}_{ab}$. This boundary condition is enforced as a Bjorhus condition on $u^{\hat{1}-}_{ab}$,

$$P^{(P)cd}_{ab} d_t u^{\hat{1}-}_{cd} = P^{(P)cd}_{ab} [D_t u^{\hat{1}-}_{cd} - (N + n_k N^k) w^-_{cd}], \quad \text{(E31)}$$

which is the same condition used in the pure GH Einstein system case [7]. Higher-order physical boundary conditions have also been derived for the pure GH Einstein system [18], and these could be used, essentially without modification, for the GH Einstein gauge-driver system as well.

[1] L. Lindblom, K. D. Matthews, O. Rinne, and M. A. Scheel, Phys. Rev. D **77**, 084001 (2008).
[2] F. Pretorius, Phys. Rev. Lett. **95**, 121101 (2005).
[3] F. Pretorius, Classical Quantum Gravity **23**, S529 (2006).
[4] M. A. Scheel, M. Boyle, T. Chu, L. E. Kidder, K. D. Matthews, and H. P. Pfeiffer, Phys. Rev. D **79**, 024003 (2009).
[5] L. E. Kidder, L. Lindblom, M. A. Scheel, L. T. Buchman, and H. P. Pfeiffer, Phys. Rev. D **71**, 064020 (2005).
[6] M. Boyle, L. Lindblom, H. P. Pfeiffer, M. A. Scheel, and L. E. Kidder, Phys. Rev. D **75**, 024006 (2007).
[7] L. Lindblom, M. A. Scheel, L. E. Kidder, R. Owen, and O. Rinne, Classical Quantum Gravity **23**, S447 (2006).
[8] J. R. Dormand and P. J. Prince, J. Comput. Appl. Math. **6**, 19 (1980).
[9] F. Estabrook, H. Wahlquist, S. Christensen, B. DeWitt, L. Smarr, and E. Tsiang, Phys. Rev. D **7**, 2814 (1973).
[10] G. B. Cook and H. P. Pfeiffer, Phys. Rev. D **70**, 104016 (2004).
[11] J. P. Boyd, *Chebyshev and Fourier Spectral Methods* (Dover Publications, New York, 1999), 2nd ed.
[12] D. Gottlieb and J. S. Hesthaven, J. Comput. Appl. Math. **128**, 83 (2001), ISSN .
[13] M. A. Scheel, H. P. Pfeiffer, L. Lindblom, L. E. Kidder, O. Rinne, and S. A. Teukolsky, Phys. Rev. D **74**, 104006 (2006).
[14] M. W. Choptuik and F. Pretorius, arXiv:0908.1780.
[15] J. R. van Meter, J. G. Baker, M. Koppitz, and D.-I. Choi, Phys. Rev. D **73**, 124011 (2006).
[16] O. Rinne, L. Lindblom, and M. A. Scheel, Classical Quantum Gravity **24**, 4053 (2007).
[17] O. Rinne, Classical Quantum Gravity **23**, 6275 (2006).
[18] O. Rinne, L. T. Buchman, M. A. Scheel, and H. P. Pfeiffer, Classical Quantum Gravity **26**, 075009 (2009).